Article

Chinese Science Bulletin

SPECIAL ISSUE: Nano-Biomedical Optoelectronic Materials and Devices
Progress of Projects Supported by NSFC

July 2013 Vol.58 No.21: 2606–2610
doi: 10.1007/s11434-012-5549-5

Selectable infiltrating large hollow core photonic band-gap fiber

LIU JianGuo[1*], DU YuanXin[1], ZHU NingHua[1] & LIU FengMei[2]

[1] *State Key Laboratory of Integrated Optoelectronics, Institute of Semiconductors, Chinese Academy of Sciences, Beijing 100083, China;*
[2] *Haidian Maternal & Child Health Hospital, Beijing 100080, China*

Received February 17, 2012; accepted August 30, 2012; published online November 23, 2012

A selectable infiltrating large hollow core photonic band-gap fiber is fabricated with simple arc discharge technique. The offset, discharge duration, arc current and discharge times are optimized for selected sealing side air-holes but leave the central large air-hole partially open. The collapse length of the PCF is shortened by increasing the number of discharges and offset with discharge duration and arc current kept at a relatively low level. Light with the wavelength located at the photonic band-gap can still propagate while the central hollow air-hole is infiltrated with a kind of oil with refractive index of 1.30. The selectable infiltrating large hollow core photonic band-gap fiber has potential application for implementing novel lasers, sensors and tunable optoelectronic devices.

photonic band-gap fiber, side air-hole sealing, infiltration

Citation: Liu J G, Du Y X, Zhu N H, et al. Selectable infiltrating large hollow core photonic band-gap fiber. Chin Sci Bull, 2013, 58: 2606–2610, doi: 10.1007/s11434-012-5549-5

Photonic crystal fibers (PCFs) have attracted strong interest due to such salient features as endless single-mode transmission, flexible chromatic dispersion, large mode area, high nonlinearity, etc. [1–18]. Due to their flexible structures, PCFs have been used for a number of fiber-optic devices—such as optical switches, wavelength converters, high-power fiber lasers, supercontinuum light sources, and gas sensors etc.—that are difficult to achieve using conventional fibers [19–21]. Another merit of PCFs is that they provide a platform for filling rare-earth ions, liquid crystal, gas or liquid solution into their hollow air holes [22–46].

The band-gap guiding mechanism is usually maintained when air-holes are filled with gases because the PCF's transverse refractive index distribution is almost unchanged. But the band-gap usually shifts substantially or disappears when liquid infiltrates into the air-holes because the PCF's refractive index distribution is changed. Therefore, in order to let liquid infiltrate into the hollow core but preserve the band-gap guiding mechanism, the side air-holes of the hollow core PCF have to be sealed. To our knowledge, there have been three methods to achieve the selective sealing and filling: (I) The central hollow core is filled by means of differential filling speed that depends on the size of the air holes [21], but the UV curable polymer and a multi-step injection-cure-cleave process make this method complicated. (II) The side air-holes are sealed by splicing with a single-hole hollow-core fiber [22]. The matching single hollow core fiber and the accurate cleaving limits the usefulness of this method. (III) The side air-holes are collapsed with arc fusion technique [23–25]. The injection-cure-cleave process and the UV curable polymer renders this method impractical. So how to selectively seal the side air-holes and fill hollow core of PCF remains a major technical challenge.

In this paper, we used an improved Method III to seal the side air-holes of a large hollow core PCF. Multiple arc discharges are dispensed to compensate for the discharge energy decline due to the increased offset. The collapse length of the PCF is shortened by increasing the number of discharges and offset with the discharge duration and the arc current kept at relative low level. To verify the disposed

*Corresponding author (email: jgliu@semi.ac.cn)

PCF can be used for liquid infiltration, a kind of refractive index oil with index of 1.30 is filled into the hollow center air holes. In our experiment, light can propagate through the liquid filled PCF successfully with about 6.5 dB total loss.

Our experimental process consists of three steps. Step 1: Sealing—the side air-holes of a large core PCF are sealed with the large central air-holes partially open; Step 2: Infiltration—in order to demonstrate the photonic band-gap propagation mechanism, a kind of liquid refractive index oil with refractive index less than that of silica is infiltrated into the central hollow core of the PCF; Step 3: Measurement—the transmission characters of the liquid core PCF are measured. It is indicated that the guiding mechanism is photonic band-gap when light transmits through the liquid core PCF because the effective index of the core is less than that of the cladding.

1 Selected sealing the side air-holes

1.1 Sample

Figure 1 shows the transverse scan electronic microscope (SEM) of HC19-1550-01 photonic band-gap fiber. Its center operating wavelength, attenuation at center operating wavelength, width of transmission band, fraction of light propagating in air, mode field diameter, numerical aperture and effective mode index are 1570 nm, less than 0.02 dB/m, more than 80 nm, more than 97%, 13 μm, 0.13 and 0.995, respectively. The core diameter, pitch, air filling fraction in the holey region, diameter of holey core region, diameter of silica cladding and coating diameter are almost 20 μm, 3.9 μm, larger than 90%, 73 μm, 115 μm, 200 μm, respectively.

1.2 Sealing

Figure 2 shows the schematic of the arc discharge. l is the offset and it is defined as the space from the axis of the two electrodes to the tip of the PCF. In our experiment, a Fujikura FSM-40s Arc Fusion Splicer is used. The arc current, discharge duration, offset and number of discharges are adjusted to seal the side air-holes. The key parameters of the ARC Fusion Splicer are listed in Table 1.

A traditional single mode fiber (SMF) and a PCF sample are placed in the splicer, after auto adjustment; the SMF is

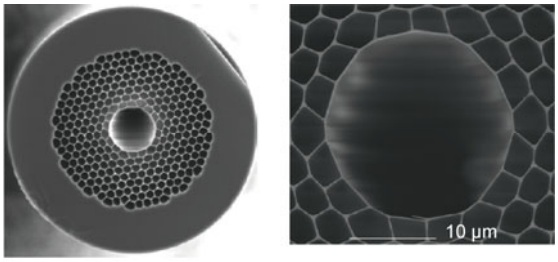

Figure 1 The transverse SEM of HC19-1550-01 type PCF.

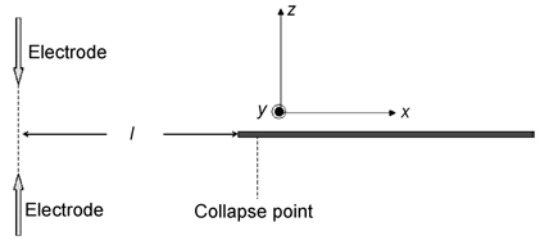

Figure 2 The schematic of arc discharge.

Table 1 The parameters of the arc fusion splicer

Parameters	Values/status
Mode title	Manual splice
Fiber type	Special
Cleaning arc	180 ms
Gap	10 μm
Overlap	10 μm
Prefuse power	20 bit
Prefuse time	180 ms
Arc power	20 bit
Arc time	2000 ms
MFD-L	9.3 μm
MFD-R	9.3 μm
Core curve	100
Minimum loss	0.00 dB
Core step	100

removed before the start of the arc discharge; the end of the PCF sample is heated by an arc discharge without splicing with the SMF. The current density distribution [25] between two electrodes is

$$I(r,z)=\frac{I_0}{2\pi\sigma(z)^2}\exp\left(-\frac{r^2}{2\sigma(z)^2}\right). \quad (1)$$

The coordinates x, y, z are defined in Figure 2. $r^2=x^2+y^2$. I_0 is the total current, $\sigma(z)$ is the Gaussian width of the current density at position z, and can be written as $\sigma(z)=\sigma_0(1+Cz^2)^{-1/3}$. σ_0 is the Gaussian width of the current density at the midpoint of the electrodes separation (z=0); C is a constant determined from the variation of the square of the current density in the z direction. The energy density changes with the square of the discharge current and discharge duration, and the temperature is proportional to the energy density. From eq. (1), the current decreases when the offset increases. When the temperature of heated fiber exceeds the softening point at around 1670°C, the surface tension will overcome the viscosity and cause the PCF's cylindrical air holes collapse. The collapse point is defined as the location at which the temperature reaches the softening point. The collapse length is defined as the space from the collapse point to the collapse tip of the PCF. The rate [21]

of collapse is

$$V_{\text{collapse}} = \gamma / 2\eta, \quad (2)$$

where γ is the surface tension of silica, which is almost a constant. η is the viscosity of silica, which decreases sharply with increasing temperature, so the air holes collapse very quickly in the high temperature region. Eqs. (1) and (2) suggest that increasing offset can shorten the collapse length, and the decline of the discharge energy can be compensated by increasing the discharge times.

2 Infiltration process and measurement setup

2.1 Infiltration process

After both sides of the PCF are sealed, a kind of refractive index oil with refractive index of 1.30 is infiltrated into the central core of the PCF. We use a medical injector to accelerate the infiltration process. The experimental setup scheme and picture are shown in Figure 3. One side of the PCF is dipped into the refractive index oil. The other side is incorporated into the injector. The port of the injector is sealed by an unguent, which can be easily removed from the PCF after the infiltration process. The piston of the injector is pulled to make the air pressure in the injector (one side of PCF) far lower than that in the refractive index oil (the other side of PCF). So the liquid infiltration process is accelerated beyond capillary action.

2.2 Measurement setup

Figure 4 shows the measurement setup. A DFB laser with center wavelength of 1550 nm and an EDFA are used as the light sources; a power meter and an optical spectra analyzer (OSA) with resolution of 0.01 nm are used as the detectors. In our experiment, the PCF incorporated into a bare fiber adaptor is connected to an SMF without splicing.

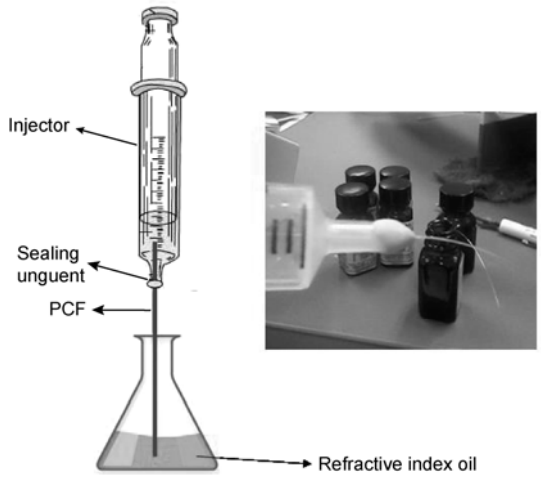

Figure 3 The infiltration experimental setup.

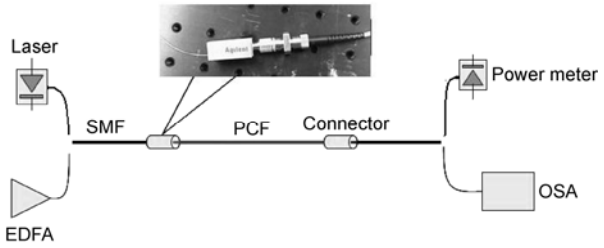

Figure 4 Measurement setup.

3 Results

Figure 5 shows the side picture of the sealed PCF (left) and SMF (right). The offset, arc duration and arc current are 40 μm, 500 ms and 15 mA, respectively. It can be seen from the figure that the side air-holes of the PCF are sealed perfectly with the central air-hole partially open, but almost no power is detected when the refractive index oil is infiltrated into the open core. The reason is that the collapse length is too long and the light power emitted from a SMF is not effectively coupled into the center core of the liquid filled PCF because of diffraction effect.

In order to shorten the collapse length, the offset is increased. At the same time, the arc duration or arc current is enhanced so that the declined discharge energy is compensated. Figure 6 shows the side picture of the sealed PCF with different offsets, arc durations and arc currents. It can be seen that the collapse length is not shortened by increasing the offset when the discharge duration or arc current is increased. This results in the collapse point (Figure 2) shift to the right when the arc current increases, as can be seen from eq. (1). The soften point also will shift to the right when the discharge duration increases because of the thermal conduction.

In order to shorten the collapse length, we increase the number of discharges to compensate for the increased offset induced discharge energy decline but with the arc duration or arc current kept at a relatively low level. The fiber will get cold after each discharge. This avoids the collapse range extending due to the thermal conduction. Figure 7 shows the side picture for different number of discharges without changing the sealing arc duration and arc current. It can be seen from the figure that the side air-holes collapse when the number of discharges increases. All the side air-holes are closed when discharge time is 4; the SEM picture is shown in Figure 8. Comparing Figure 7(c) with Figure 6(a), the collapse length decreases significantly simply by increasing the number of discharges with a lower arc duration

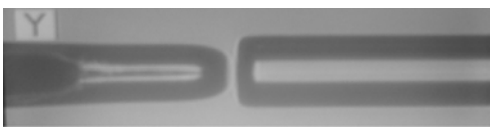

Figure 5 The side picture of the fusion side.

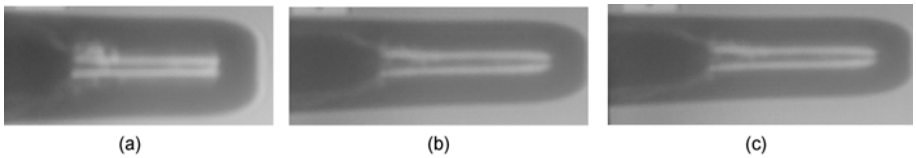

Figure 6 The side picture of the side air-holes sealed PCF with different offsets, discharge durations and arc currents. The offset, discharge duration, arc current are 100 μm, 1000 ms, 20 mA (a); 80 μm, 600 ms, 18 mA (b); and 40 μm, 500 ms, 15 mA (c).

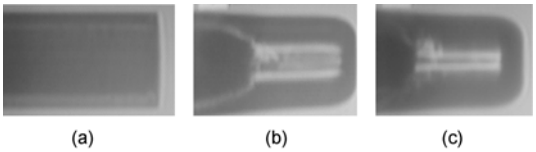

Figure 7 The side pictures for different number of discharges. (a) Original, (b) 2 times and (c) 4 times with offset, discharge duration, arc current of 100 μm, 500 ms, 15 mA.

and lower arc current.

Figure 9 shows relative transmitted power varies with the different discharge times when offset, arc duration, arc current transmitting power are 120 μm, 1000 ms, 15 mA, respectively. P_0 is the original when 1-m PCF is directly connected with the laser and the power meter. P is the detected power when the side air-holes are selected sealed and the center hollow air-holes are filled with the refractive index oil. The corresponding optical spectra are plotted in Figure 10. It can be seen from the figures that light successfully transmits through the liquid filled PCF. Because the refractive index of the core is smaller than the cladding, the photonic bandgap guiding mechanism is preserved. In our experiment, about 6.5 dB total loss is achieved.

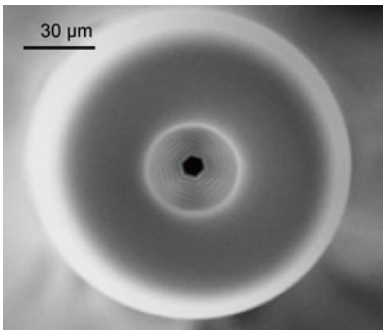

Figure 8 The transverse SEM when the discharge time is 4.

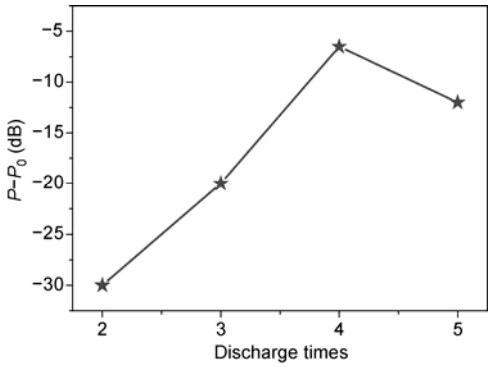

Figure 9 The relative transmitted power with different discharge times when offset, arc duration, arc current are 120 μm, 1000 ms, 15 mA, respectively.

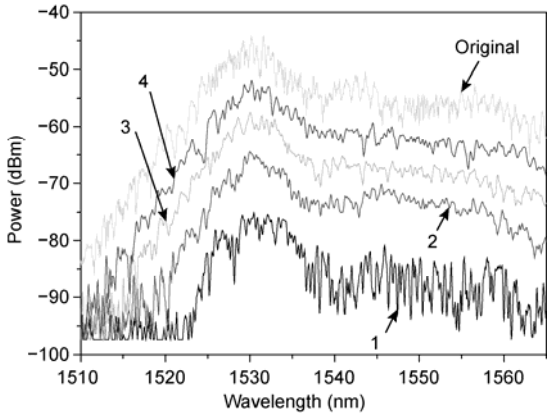

Figure 10 The spectra of different discharge times with offset, arc duration, arc current of 120 μm, 1000 ms, 15 mA.

4 Conclusions

The side air-holes of a large hollow core PCF are selectively sealed with the central air-hole partially open using arc discharge technique. The number of discharges and offset increase with the discharge duration, and arc current is kept at a relatively low level to shorten the collapse length of the PCF. The results provide a practical way of selectively sealing and filling the PCF with liquid for implementing novel lasers, sensors and tunable devices.

This work was supported by the State Key Program of National Natural Science Foundation of China (61036012), the National Basic Research Program of China (2012CB315702), the National Natural Science Foundation of China (61177060), the Major Program of the National Natural Science Foundation of China (61090390), the Innovative Research Groups of the National Natural Science Foundation of China (61021003), and the International Cooperation and Exchange of the National Natural Science Foundation of China (60820106004).

1 Liu J G, Kai G Y, Xue L F, et al. Modal cutoff properties in germanium-doped photonic crystal fiber. Appl Optics, 2006, 45: 2035–2038
2 Liu J G, Xue L F, Kai G Y, et al. Mode exiting properties of photonic crystal fiber with optical field incident from a single mode fiber. Chin Phys Lett, 2006, 23: 2125–2128

3 Liu J G, Xue L F, Liu Y G, et al. Enhanced nonlinearity in a simultaneously tapered and Yb^{3+}-doped photonic crystal fiber. J Opt Soc Am B, 2006, 23: 2448–2453
4 Liu J G, Kai G Y, Zhang C S, et al. Conditions for higher-order resonant modes to be excited in a photonic-crystal fiber Bragg grating. J Opt Soc Am B, 2006, 23: 370–374
5 Liu J G, Xue L F, Wang Z, et al. Large anomalous dispersion at short wavelength and modal properties of a photonic crystal fiber with large air holes. IEEE J Quant Electron, 2006, 42: 961–968
6 Liu J G, Xue L F, Wang Y J, et al. Impacts of imperfect geometry structure on the nonlinear and chromatic dispersion properties of a microstructure fiber. Appl Optics, 2007, 46: 7771–7775
7 Li Y, Liu J G, Kai G Y, et al. The effect of irregular structure to birefraction in a photonic crystal fiber. Chin Phys Lett, 2007, 24: 2879–2882
8 Wang Z, Liu Y G, Kai G Y, et al. Directional couplers operated by resonantcoupling in all-solid photonic bandgap fibers. Opt Exp, 2007, 15: 8925–8930
9 Zhang C S, Kai G Y, Wang Z, et al. Simulations of effect of high-index materials on highly birefringent photonic crystal fibres. Chin Phys Lett, 2005, 22: 2858–2861
10 Jin L, Kai G Y, Li J Y, et al. Fibre Bragg gratings inscribed in homemade microstructured fibres. Chin Phys Lett, 2007, 24: 61603–61606
11 Yue Y, Kai G Y, Wang Z, et al. Phase and group modal birefringence of an index-guiding photonic crystal fibre with helical air holes. Optics Commun, 2006, 268: 46–50
12 Yue Y, Kai G Y, Wang Z, et al. Highly birefringent elliptical-hole photonic crystal fiber with squeezed hexagonal lattice. Opt Lett, 2007, 32: 469–471
13 Yue Y, Kai G Y, Wang Z, et al. Highly birefringent elliptical-hole photonic crystal fiber with two big circular air holes adjacent to the core. IEEE Photon Technol Lett, 2006, 18: 2638–2640
14 Yue Y, Kai G, Wang Z, et al. Broadband single-polarization single-mode photonic crystal fiber coupler. IEEE Photon Technol Lett, 2006, 18: 2032–2034
15 Jin L, Guan B O, Fang Q, et al. Bragg gratings written in photonic crystal fibres with a high-index germanosilicate core. Chin Phys Lett, 2008, 25: 160–163
16 Liu J G, Cheng T H, Yeo Y K, et al. Light beam coupling between standard single mode fibers and high nonlinearly photonic crystal fibers based on fused biconical tapered technique. Opt Exp, 2009, 17: 11766–11772
17 Liu J G, Kai G Y, Xue L F, et al. An all-optical switching based on highly nonlinear photonic crystal fiber Sagnac loop mirror. Acta Phys Sin, 2007, 56: 941–945
18 Liu J G, Cheng T H, Yeo Y K, et al. Stimulate brillouin scattering based broadband tunable low-light conversion in a highly nonlinear photonic crystal fiber. J Lightwave Technol, 2009, 27: 1279–1285
19 Liu J G, Cheng T H, Yeo Y K, et al. All-optical continuously tunable delay with a high linear-chirp-rate fiber Bragg grating based on four-wave mixing in a highly-nonlinear photonic crystal fiber. Optics Commun, 2009, 282: 4366–4369
20 Larsen T, Bjarklev A, Hermann D, et al. Optical devices based on liquid crystal photonic bandgap fibres. Opt Exp, 2003, 11: 2589–2596
21 Huang Y, Xu Y, Yariv A. Fabrication of functional microstructured optical fibers through a selective filling technique. Appl Phys Lett, 2004, 85: 5182–5184
22 Martelli C, Canning J, Lyytikainen K, et al. Water-core fresnel fiber. Opt Exp, 2005, 13: 3890–3895
23 Yiou S, Delaye P, Rouvie A, et al. Stimulated raman scattering in an ethanol core microstructured optical fiber. Opt Exp, 2005, 13: 4786–4791
24 Nielsen K, Noordegraaf D, Sorensen T, et al. Selective filling of photonic crystal fibres. J Opt A: Pure Appl Opt, 2005, 7: L13–L20
25 Xiao L M, Jin W, Demokan M S, et al. Fabrication of selective injection microstructured optical fibers with a conventional fusion splicer. Opt Exp, 2005, 13: 9014–9022
26 Kunimasa S, Nikolaos F, Varshney, et al. Tunable photonic crystal fiber couplers with a thermo-responsive liquid crystal resonator. IEEE/OSA J Lightwave Technol, 2008, 26: 663–669
27 Alkeskjold T, Lægsgaard J, Bjarklev A. All-optical modulation in dye-doped nematic liquid crystal photonic bandgap fibers. Opt Exp, 2004, 12: 5857–5871
28 Yu C P, Liou J H, Huang S S, et al. Tunable dual-core liquid-filled phtonic crystal fibers for dispersion compensation. Opt Exp, 2008, 16: 4443–4451
29 Chugreev A, Nazarkin A, Abdolvand A, et al. Manipulation of coherent stokes light by transient stimulated Raman scattering in gas filled hollow-core PCF. Opt Exp, 2009, 17: 8822–8829
30 Du J B, Liu Y G, Wang Z, et al. Thermally tunable dual-core photonic bandgap fiber based on the infusion of a temperature-responsive liquid. Opt Exp, 2008, 16: 4263–4269
31 Noordegraaf D, Scolari L, Lægsgaard J, et al. Electrically and mechanically induced long period gratings in liquid crystal photonic bandgap fibers. Opt Exp, 2007, 15: 7901–7912
32 Fedotov I V, Fedotov A B, Zheltikov A M. Raman-resonance-enhanced composite nonlinearity of air-guided modes in hollow photonic-crystal fibers. Opt Lett, 2006, 31: 2604–2606
33 Ma J J, Bock W J. Modeling of photonic crystal fiber with air holes sealed at the fiber end and its application to fluorescent light collection efficiency enhancement. Opt Exp, 2005, 13: 2385–2393
34 Yu C P, Liou J H. Selectively liquid-filled photonic crystal fibers for optical devices. Opt Exp, 2009, 17: 8729–8734
35 Domachuk P, Nguyen H C, Eggleton B J, et al. Microfluidic tunable photonic bandgap device. Appl Phys Lett, 2004, 84: 1838–1840
36 Gundu K M, Kolesik M, Moloney J V, et al. Ultra-flattened-dispersion selectively liquid-filled photonic crystal fibers. Opt Exp, 2006, 14: 6870–6878
37 Du F, Lu Y Q, Wu S T. Electrically tunable liquid-crystal photonic crystal fiber. Appl Phys Lett, 2004, 85: 2181–2183
38 Noordegraaf D, Scolari L, Lægsgaard J, et al. Electrically and mechanically induced long period gratings in liquid crystal photonic bandgap fibers. Opt Exp, 2007, 15: 7901–7912
39 Noordegraaf D, Scolari L, Lægsgaard J. Avoided-crossing-based liquid-crystal photonic-bandgap notch filter. Opt Lett, 2008, 33: 986–988
40 Zhang R, Teipel J, Giessen H. Theoretical design of a liquid-core photonic crystal fiber for supercontinuum generation. Opt Exp, 2006, 14: 6800–6812
41 Fini J M. Microstructure fibres for optical sensing in gases and liquids. Meas Sci Technol, 2004, 15: 1120–1128
42 Jensen J B, Pedersen L H, Hoiby P E, et al. Photonic crystal fiber based evanescent-wave sensor for detection of biomolecules in aqueous solutions. Opt Lett, 2004, 29: 1974–1976
43 Kerbage C, Steinvurzel P, Reyes P, et al. Highly tunable birefringent microstructured optical fiber. Opt Lett, 2002, 27: 842–844
44 Benabid F, Couny F, Knight J C, et al. Compact, stable and efficient all-fibre gas cells using hollow-core photonic crystal fibres. Nature, 2005, 434: 488–491
45 Benabid F, Bouwmans G, Knight J C, et al. Ultrahigh efficiency laser wavelength conversion in a gas-filled hollow core photonic crystal fiber by pure stimulated rotational Raman scattering in molecular hydrogen. Phys Rev Lett, 2004, 93: 123903
46 Monro T M, Belardi W, Furusawa K, et al. Sensing with microstructured optical fibres. Meas Sci Technol, 2001, 12: 854–858